

Initial Use of Dioximate Ligands in 3d/4f Cluster Chemistry: Synthesis, Structure, and Magnetic Studies of an Unusual $[\text{Gd}^{\text{III}}_2\text{Mn}^{\text{IV}}\text{O}]^{8+}$ Complex

Christos Lampropoulos, Theocharis C. Stamatatos, Khalil A. Abboud, and George Christou*

Department of Chemistry, University of Florida, Gainesville, Florida 32611-7200

Received October 20, 2008

An unusual $[\text{Mn}^{\text{IV}}\text{Gd}^{\text{III}}_2(\mu_3\text{-O}^{2-})]^{8+}$ triangular complex has been prepared from the initial use of 2,6-diacetylpyridine dioxime (dapdoH₂) in 3d/4f cluster chemistry. The complex has an $S = 13/2$ ground state, with exchange parameters $J = +0.49 \text{ cm}^{-1}$ and $J' = -0.12 \text{ cm}^{-1}$ [$\mathcal{H} = -2J(\hat{S}_i \cdot \hat{S}_j)$ convention] for the $\text{Gd}^{\text{III}} \cdots \text{Mn}^{\text{IV}}$ and $\text{Gd}^{\text{III}} \cdots \text{Gd}^{\text{III}}$ interactions, respectively. The origin of this ground state has been rationalized by consideration of the spin frustration occurring within the complex as a function of the relative magnitude of the competing interactions.

Intense attention has been directed in the recent years toward the synthesis of polynuclear 3d metal clusters.¹ This field has particularly flourished because of the realization that such molecular species will often possess very interesting magnetic properties and that some of them are single-molecule magnets (SMMs). SMMs are molecules that function as magnets below a critical temperature, providing a new “bottom-up” approach to nanoscale magnetic materials.² Several groups have since explored mixed 3d/4f compounds, and particularly Mn/Ln ones, as attractive routes to new SMMs, encouraged by the report of a Cu_2Tb_2 SMM by Matsumoto and co-workers.³ The hope has been that a lanthanide’s often significant spin and/or its often large anisotropy will lead to 3d/4f SMMs with properties significantly different from those of homometallic 3d ones. Indeed, this approach has successfully led to several Mn/Ln SMMs, including $\text{Mn}_{11}\text{Ln}_4$,⁴ $\text{Mn}_{11}\text{Gd}_2$,⁵ Mn_5Ln_4 ,⁶ and Mn_6Dy_6 ⁷ examples.

* To whom correspondence should be addressed. E-mail: christou@chem.ufl.edu.

- (1) Winpenny, R. E. P. In *Comprehensive Coordination Chemistry II*; McCleverty, J. A., Meyer, T. J., Eds.; Elsevier: Amsterdam, The Netherlands, 2004; Vol. 7, pp 125–175.
- (2) For a review, see: Christou, G. *Polyhedron* **2005**, *24*, 2065, and references cited therein.
- (3) Osa, S.; Kido, T.; Matsumoto, N.; Re, N.; Pochaba, A.; Mrozinski, J. *J. Am. Chem. Soc.* **2004**, *126*, 420.
- (4) Mishra, A.; Wernsdorfer, W.; Abboud, K. A.; Christou, G. *J. Am. Chem. Soc.* **2004**, *126*, 15648.
- (5) Mereacre, V. M.; Ako, A. M.; Clerac, R.; Wernsdorfer, W.; Filoti, G.; Bartolome, J.; Anson, C. E.; Powell, A. K. *J. Am. Chem. Soc.* **2007**, *129*, 9248.
- (6) Mereacre, V.; Ako, A. M.; Clerac, R.; Wernsdorfer, W.; Hewitt, I. J.; Anson, C. E.; Powell, A. K. *Chem.—Eur. J.* **2008**, *14*, 3577.

The Mn/Ln complexes obtained to date have not usually been amenable to detailed studies that can yield the magnitudes of the intramolecular exchange interactions and a resulting rationalization of how these lead to the observed ground state S value. Reasons for this are varied and include (i) the usually high nuclearity of these molecules and the consequently large number of pairwise exchange interactions (J_{ij}), many of which are competing and lead to spin frustration effects, (ii) the weak nature of the Mn–Ln and Ln–Ln exchange interactions, and (iii) spin–orbit coupling effects, which preclude accurate magnetic susceptibility fits for polynuclear systems.⁸ For such reasons, we are targeting new synthetic routes that might yield small-nuclearity Mn/Ln complexes that are more amenable to an analysis of the sign and nature of their exchange interactions. We have recently been employing 2,6-diacetylpyridine dioxime (dapdoH₂) in 3d/4f chemistry, and we can report that this has led to a new $\text{Gd}^{\text{III}}_2\text{Mn}^{\text{IV}}$ complex with an unusual mix of metal oxidation states; we herein describe the synthesis, structure, and magnetochemical characterization of this compound. This also represents the initial use of dapdoH₂ in mixed-metal cluster chemistry, having been employed to date only in homometallic $\text{Mn}^{\text{II/III}}$ ⁹ and heterometallic $\text{Cr}^{\text{III}}\text{—Cu}^{\text{II}}$ ¹⁰ complexes.

The reaction of $\text{Mn}(\text{O}_2\text{CPh})_2 \cdot 2\text{H}_2\text{O}$, $\text{Gd}(\text{NO}_3)_3 \cdot 6\text{H}_2\text{O}$, dapdoH₂, and NEt_3 in a 1:1:2:4 molar ratio in MeCN gave a dark-brown solution, from which were subsequently isolated brown crystals of $[\text{MnGd}_2\text{O}(\text{O}_2\text{CPh})_3(\text{O}_2\text{CMe})(\text{dapdo})(\text{dapdoH}_2)]$ (**1**) in 60% yield as $1 \cdot 10\text{MeCN}$.¹¹ The acetate anion very likely comes from Mn^{III} - or Mn^{IV} -catalyzed aerial oxidation of MeCN. Dried

- (7) Zaleski, C. M.; Depperman, E. C.; Kampf, J. W.; Kirk, M. L.; Pecoraro, V. L. *Angew. Chem., Int. Ed.* **2004**, *43*, 3912.
- (8) Panagiotopoulos, A.; Zafiroopoulos, Th. F.; Perlepes, S. P.; Bakalbassis, E.; Masson-Ramade, I.; Kahn, O.; Terzis, A.; Raptopoulou, C. P. *Inorg. Chem.* **1995**, *34*, 4918.
- (9) Stamatatos, T. C.; Luisi, B. S.; Moulton, B.; Christou, G. *Inorg. Chem.* **2008**, *47*, 1134.
- (10) Khanra, S.; Weyhermuller, T.; Chaudhuri, P. *Dalton Trans.* **2008**, 4885.
- (11) Anal. Calcd (found) for dried **1** (solvent-free): C, 48.74 (48.62); H, 4.34 (4.39); N, 10.23 (10.09). Crystal structure data for $1 \cdot 10\text{MeCN}$: $\text{C}_{70}\text{H}_{75}\text{Gd}_2\text{MnN}_9\text{O}_{15}$, 1791.93 g mol⁻¹, monoclinic, *I*2/a, $a = 19.424(2) \text{ \AA}$, $b = 27.132(3) \text{ \AA}$, $c = 30.071(3) \text{ \AA}$, $\beta = 90.155(2)^\circ$, $Z = 8$, $V = 15848(3) \text{ \AA}^3$, $d_{\text{calc}} = 1.502 \text{ g cm}^{-3}$, $T = 173(2) \text{ K}$. Final R1 = 8.87 and wR2 = 19.76.

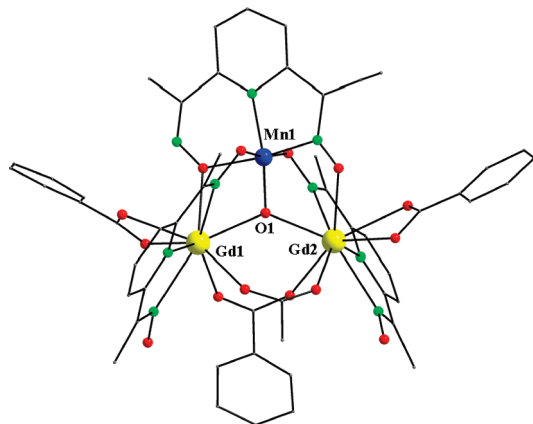


Figure 1. Molecular structure of **1**. Color code: Mn^{IV}, blue; Gd^{III}, yellow; O, red; N, green; C, gray. Hydrogen atoms are omitted for clarity.

solid analyzed satisfactorily (C, H, and N) as solvent-free,¹¹ ruling out the possibility that the acetate is in reality a NO₃[−] group; the same reaction in a different solvent does not give complex **1**. The structure of **1** (Figure 1) consists of an isosceles Gd^{III}₂Mn^{IV} triangle with a central μ₃-O^{2−} ion O1, which is slightly (0.034 Å) above the MnGd₂ plane. Each dapdoH[−] group is a tridentate chelate on a Gd atom and forms a diatomic Gd–N–O–Mn bridge to Mn1 with its deprotonated NO[−] arm. The dapdo^{2−} group is a tridentate chelate on Mn1 and bridges asymmetrically to the Gd atoms: one NO[−] arm forms a diatomic Mn–N–O–Gd bridge to one Gd atom, whereas the other forms a monatomic Mn–O–Gd bridge to the other Gd atom. This asymmetric bridging mode is statically disordered in the crystal. The Gd⋯Gd edge is bridged by a benzoate and an acetate group. Ligation is completed by a chelating (η²) benzoate group on each Gd atom. The Mn^{IV} oxidation state and O^{2−} protonation level were established by bond valence sum (BVS) calculations,¹² charge considerations, and inspection of the metric parameters. Mn1 is six-coordinate with distorted octahedral geometry, whereas each Gd³⁺ ion is nine-coordinate with a distorted capped square-antiprismatic geometry. Compound **1** is the first Mn/Ln complex with a triangular topology and the first 3d/4f cluster with a dioximate ligand.

Solid-state direct current magnetic susceptibility (χ_M) data on dried **1** were collected in a 1 kG (0.1 T) field in the 5.0–300 K range and are plotted as χ_MT vs T in Figure 2. χ_MT has a value of 17.60 cm³Kmol^{−1} at 300 K, and it remains essentially constant down to 50 K and then rapidly increases to 23.62 cm³Kmol^{−1} at 5 K. The χ_MT value at 300 K is essentially the same as the spin-only (g = 2) value of 17.64 cm³Kmol^{−1} for one Mn^{IV} (S = 3/2) and two Gd^{III} (S = 7/2, L = 0) noninteracting ions. The essentially constant value down to 50 K is consistent with very weak exchange interactions in the molecule, as expected when Ln ions are involved. To determine the individual pairwise exchange parameters J and J' between the Gd–Mn and Gd–Gd pairs, respectively, the χ_MT vs T data were fit to the appropriate theoretical expression for an isosceles Gd^{III}₂Mn^{IV} triangle of C_{2v}

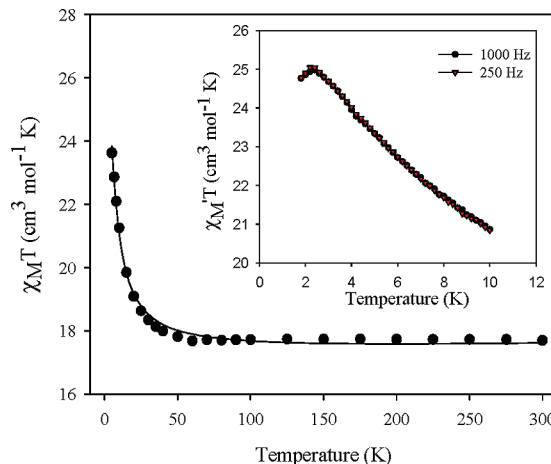


Figure 2. χ_MT vs T plot for complex **1** in a 1 kG field. The solid line is the fit of the data to the theoretical expression; see the text for the fit parameters. Inset: Plot of the in-phase ac susceptibility (χ'_M, as χ'_MT) of **1** in a 3.5 G field oscillating at the indicated frequencies.

symmetry; i.e., we assumed that the Gd–Mn interactions would be very weak and essentially identical despite the slightly different bridges described above. The isotropic spin Hamiltonian describing the exchange interactions within **1** is given by eq 1, where \hat{S}_i is the spin operator for metal atom M_i (i = 1 for Mn and 2 and 3 for Gd).

$$\mathcal{H} = -2J(\hat{S}_1 \cdot \hat{S}_2 + \hat{S}_1 \cdot \hat{S}_3) - 2J'\hat{S}_2 \cdot \hat{S}_3 \quad (1)$$

The eigenvalues of this spin Hamiltonian can be determined analytically with the Kambe vector coupling method.¹³ Thus, using the substitutions $\hat{S}_A = \hat{S}_2 + \hat{S}_3$ and $\hat{S}_T = \hat{S}_A + \hat{S}_1$, where S_T is the total spin of the molecule, allows the spin Hamiltonian to be transformed into the equivalent form given by eq 2. The eigenvalues of eq 2 are given by eq 3, where E(S_T, S_A) is the energy of state S_T arising from S_A, and constant terms contributing to all states have been omitted.

$$\mathcal{H} = -2J(\hat{S}_T^2 - \hat{S}_A^2 - \hat{S}_1^2) - 2J'(\hat{S}_A^2 - \hat{S}_2^2 - \hat{S}_3^2) \quad (2)$$

$$E(S_T, S_A) = -J[S_T(S_T + 1) - S_A(S_A + 1)] - J'[S_A(S_A + 1)] \quad (3)$$

For complex **1**, the overall multiplicity of the spin system is 256, made up of 28 spin states ranging from S_T = 1/2 to 17/2. Derivation of the appropriate Van Vleck equation and its use to fit the χ_MT vs T data (shown as the solid line in Figure 2) gave J = +0.49(2) cm^{−1}, J' = −0.12(3) cm^{−1}, and g = 1.98(1). A temperature-independent paramagnetism term was included and held constant at 900 × 10^{−6} cm³ mol^{−1}.^{8,14} The exchange interactions are thus both very weak, and of different sign, and predict the complex to have an intermediate S_T = 13/2 ground state, the |S_T, S_A⟩ = |13/2, 5⟩ state, with low-lying S_T = 11/2 and 15/2 excited states at 5.32 and 5.62 cm^{−1}, respectively, above the ground state.

In order to confirm the ground state of **1**, alternating current (ac) magnetic susceptibility studies were performed in the 1.8–10 K temperature range using a 3.5 G ac field oscillating at 250–1000 Hz. The in-phase χ'_MT signal (inset

(12) Liu, W.; Thorp, H. H. *Inorg. Chem.* **1993**, *32*, 4102. BVS values for the Mn⁴⁺ and O^{2−} ions were 3.91 and 1.97, respectively.

(13) Kambe, K. *J. Phys. Soc. Jpn.* **1950**, *5*, 48.

(14) Tasiopoulos, A. J.; Milligan, P. L.; Abboud, K. A.; O'Brien, T. A.; Christou, G. *Inorg. Chem.* **2007**, *46*, 9678.

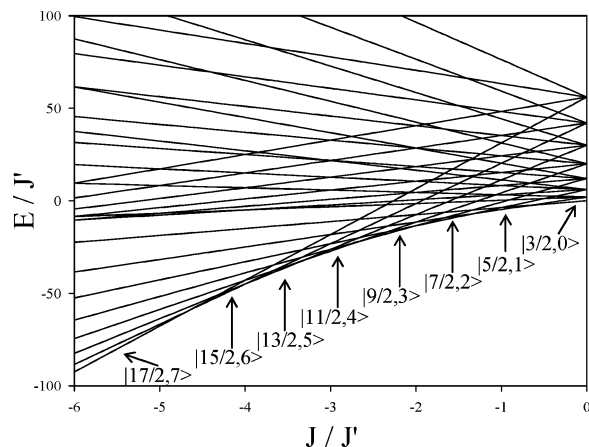


Figure 3. Variation of the spin-state energies of **1** with the J/J' ratio, showing multiple changes in the ground state; the states are labeled as $|S_T, S_A\rangle$.

of Figure 2) rapidly increases with decreasing temperature, indicating depopulation of excited states with S values smaller than the ground state, and reaches a maximum at $25.2 \text{ cm}^3\text{Kmol}^{-1}$ before then decreasing slightly, to $24.7 \text{ cm}^3\text{Kmol}^{-1}$ at 1.8 K. The lowest temperature data thus confirm an $S = 13/2$ state with $g \sim 2$; χ_{MT} values for $S = 11/2, 13/2,$ and $15/2$ with $g = 2.0$ are 17.9, 24.4, and $31.9 \text{ cm}^3\text{Kmol}^{-1}$, respectively. There were no out-of-phase ac signals down to 1.8 K, and **1** is thus not an SMM.

A ferromagnetic $J = +0.49(2) \text{ cm}^{-1}$ and an antiferromagnetic $J' = -0.12(3) \text{ cm}^{-1}$ for the Gd–Mn and Gd–Gd interactions, respectively, indicate the presence of competing interactions and spin-frustration effects. This is consistent with the observed $S = 13/2$ ground state, which does not correspond to a simple “spin up/spin down” picture of spin alignments. Instead, this value indicates some intermediate (frustrated) alignments resulting from the competing interactions, as is also indicated by the $S_A = 5$ value of the $|S_T, S_A\rangle = |13/2, 5\rangle$ ground state.¹⁵ In such situations, the ground state is extremely sensitive to the relative magnitudes of the competing exchange interactions. Because there has been no theoretical analysis to date of the spin-state energies as a ratio of the J values in an isosceles triangle comprising one $S = 3/2$ and two $S = 7/2$ spins, we have carried one out in order to rationalize the observed ground state of **1**.

In Figure 3 are plotted the energies, in units of J' , of the 28 spin states of complex **1** as a function of the J/J' ratio, for J ferromagnetic and J' antiferromagnetic values. Several important conclusions can be drawn: (i) as expected for a spin-frustrated system, the ground state is indeed very sensitive to the J/J' ratio, with eight different ground states spanning $S_T = 3/2-17/2$ being possible for this combination of signs for J and J' ; (ii) when $J \gg J'$ and as a result $|J/J'| > \sim 4.65$, the ground state is described by $S_T = 17/2$ and $S_A = 7$, i.e., the $|17/2, 7\rangle$ state, arising from J , totally overwhelming J' , and aligning the two Gd spins parallel to the Mn spin

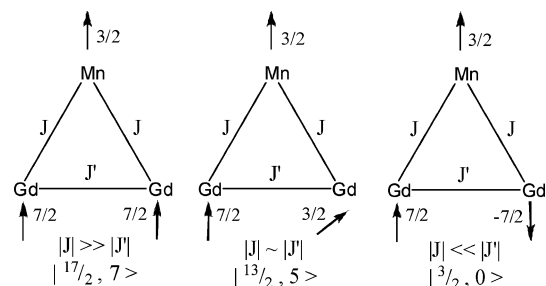


Figure 4. Depictions of the indicated $|S_T, S_A\rangle$ states, showing (left) the complete frustration of J' and the resultant $S_T = 17/2$ ground state, (middle) the intermediate situation, giving the $S = 13/2$ ground state of **1**, and (right) the complete frustration of J and the resultant $S_T = 3/2$ ground state.

and thus to each other. This is depicted in Figure 4, left, and corresponds to the antiferromagnetic J' interaction being totally frustrated. As $|J'|$ increases relative to $|J|$, the Gd spins are no longer perfectly parallel but, at some intermediate alignment, are determined by the relative magnitudes of J and J' , i.e., the $|J/J'|$ ratio. Thus, as this ratio gets progressively smaller, the Gd spins align less and less parallel and then more and more antiparallel. When $4.65 > |J/J'| > 4.2$, the ground state is $|15/2, 6\rangle$, and when $\sim 4.2 > |J/J'| > \sim 3.2$, the ground state is $|13/2, 5\rangle$, found experimentally for **1** (Figure 4, middle). Finally, when $J \ll J'$ and $\sim 0.65 > |J/J'| > 0$, the J interaction is completely frustrated, the Gd spins are perfectly antiparallel, and the ground state is thus $|3/2, 0\rangle$ (Figure 4, right).

The fit shown in Figure 2 gave $J = +0.49(2) \text{ cm}^{-1}$, $J' = -0.12(3) \text{ cm}^{-1}$, and thus $|J/J'| = 4.08$, which is within the range for a $|13/2, 5\rangle$ ground state. Note that if J and J' were (i) both ferromagnetic, (ii) antiferro- and ferromagnetic, respectively, or (iii) both antiferromagnetic, they could not yield an $S = 13/2$ ground state: the first two cases would give $S = 17/2$ and $11/2$ ground states, respectively, for all J/J' ratios, and the third could give a ground state only in the $S = 1/2-11/2$ range. Thus, although we were originally wary about the reliability of the exchange parameters obtained from the fit, it does appear that the opposite sign and relative magnitudes of J and J' are indeed correct.

In summary, a $\text{Gd}^{\text{III}}_2\text{Mn}^{\text{IV}}$ triangular complex has resulted from the initial use of a dioximate ligand in 3d/4f cluster chemistry. The complex has an $S = 13/2$ ground state, resulting from a ferromagnetic Gd^{III}–Mn^{IV} interaction and an antiferromagnetic Gd–Gd one. We are now exploring the incorporation of an anisotropic Ln^{III} ion in place of the Gd^{III} ion and the further use of dapdoH₂ in higher-nuclearity 3d/4f clusters.

Acknowledgment. This work was supported by NSF Grant CHE-0414555.

Supporting Information Available: Crystallographic data (CIF format) for **1** and structural and magnetism figures. This material is available free of charge via the Internet at <http://pubs.acs.org>.

IC802005A

(15) McCusker, J. K.; Christmas, C. A.; Hagen, P. M.; Chadha, R. K.; Harvey, D. F.; Hendrickson, D. N. *J. Am. Chem. Soc.* **1991**, *113*, 6114.